J Indian Acad Wood Sci (June 2024) 21(1):24–33
https://doi.org/10.1007/s13196-023-00329-8

ORIGINAL ARTICLE

The effect of the use of filler and recycled high-density polyethylene on the physical, mechanical and structural behavior of wood–polymer composites by the compression molding process

Charaf Lazrak[1] · **Maryama Hammi**[2]

Received: 22 February 2023 / Accepted: 7 December 2023 / Published online: 2 January 2024

Abstract In this paper, wood polymer composites (WPC) consisting of recycled high-density polyethylene and sawdust (SD) were prepared and characterized. A range of mechanical properties, including tensile strength, flexural properties, were studied, along with morphology and water contact angle. The results showed that the mechanical properties of WPC increased with an increase in 30 wt% of the SD content coupled to 7% of $CaCO_3$. Furthermore, the SD content significantly influenced the water uptake of the composites allowing good physical properties. The produced wood polymer composites also displayed an improved mechanical property with 30% of wood. Whereas a good resistance to water uptake and enhanced physical and mechanical properties are attributed to 50% of wood waste generated from wood products manufacturing such as sawdust (SD), the obtained properties have made the fabricated WPCs good potential candidates for building materials due to their improved stability and strength properties.

Keywords Recycled high-density polyethylene · Wood · Mechanical properties · Water contact angle · Morphology

✉ Charaf Lazrak
lazrakcharaf@gmail.com

Maryama Hammi
maryama.hammichimie@gmail.com

[1] Thermodynamics, Mechanics and Energetics: Experimentation, Modeling and Simulation: TME-EMS, Physical Department, Faculty of Sciences, Mohammed V University, Av Ibn Battouta, PO Box 1014, 10000 Rabat, Morocco

[2] Faculty of Sciences, Mohammed V University, Av Ibn Battouta, PO Box 1014, 10000 Rabat, Morocco

Introduction

The preservation of the forests against deforestation and waste management have led researchers to explore this waste recycling and waste from the wood–sawing industries to produce materials for multiple uses (Maraveas 2020). WPC wood– polymer composites are environmentally friendly materials, consisting essentially of a thermoplastic matrix and wood either in powder or fiber form (Friedrich 2021). They are also known as bio-based materials since the proportion of bio-ingredients can be up to 80% by volume (Roig 2018). The polymers most used in the manufacture of composites are polyvinyl chloride (PVC), polypropylene (PP) and polyethylene (PE). WPC composites have a high resistance to water and rot as solid wood (Borysiuk et al. 2020). Generally, WPC is used for exterior coatings and automotive applications, packaging for everyday needs and engineering applications (Mandal et al. 2021). The use of coupling agents in the manufacture of composites helps to strengthen the bonds between the hydrophobic matrix and the hydrophilic wood fibers. Generally, maleic anhydride polyethylene (MAPE) is used in polyethylene (PE)-based WPC at a content of up to 5% by weight (Amiandamhen et al. 2020; Kamarudin et al. 2022; Santos et al. 2021). The use of loads is also used in WPC to strengthen the structure of composites (Elamin et al. 2020). There are different manufacturing processes for composites (WPC) such as extrusion, injection molding and compression molding (Aina et al. 2022; Nur-A-Tomal et al. 2022).

The compression molding process has advantages such as high machining accuracy, low environmental impact and minimal tooling requirements (Xu et al. 2021; Ratanawilai and Srivabut 2022). This study focuses on the use of pine wood harvested from the sawmill of the Centre de

recherche forester de Rabat (Morocco) and high-density polyethylene (HDPE) derived from recycled dairy bottles and jars to produce composites based on wood–polymer panels (WPC) by the compression molding process.

The aim of this work is to shed light on the effective utilization of wood flour can minimize negative impacts on the environment, ecology and humans. The new policies for environmental issues aim to maximize the utilization of products made of fully bio-degradable materials that gives a driving force for developing the new bio-degradable materials that causes the least adverse effect on the environment and ecology.

Experimental

Starting materials

Rabat Forest Research Center's sawmill provides the maritime pine wood waste. The sawdust was dried at 103 °C for 24 h with a water content of roughly 2 to 3%, and then milled using a grinder suited to the toughness of the materials to grind and the fineness of the required powder. The sieve utilized in this study is of the size of 0.5 mm. The final granule size was determined by experiment to be between 0.1 and 0.5 mm. High-density polyethylene (HDPE) pellets were produced mostly from dairy product wastes. They underwent a thorough water wash before being dried at 65 °C for 12 h.

Preparation of the composites

The mixture of pine wood flour, recycled high-density polyethylene (HDPEr), 4% by weight of the maleic anhydride polyethylene coupling agent (MAPE) (Homkhiew et al. 2022), and calcium carbonate ($CaCO_3$) as a filler was made with a local mixer at a mixing speed of 55 tr/min for a period of 5 min in order to obtain a homogeneous mixture (Kuo et al. 2009), the resulting mat is cast into a 20 cm^2 metal mold. The pressing cycle was carried out by a press (STETON Hydraulic). The pressing process was carried out for several cycles (3–4 times) to balance the particles inside the mold, then under a temperature of T = 180 °C and a pressure of P = 6 MPa, the mat was pressed for 30 min hot from cold under the same pressure (Srivabut et al. 2018). The final size of the composite panel was 200 × 200 × 4.5 (thickness) mm. The obtained panels were conditioned at room temperature (23 ± 2 °C), with relative humidity of 50 ± 5% for at least 40 h according to ASTM D618-99 (ASTM 2002a). The formulations of wood–plastic composites are given in Table 1.

Table 1 Wood–plastic composite formulations (percentage by weight)

Samples	HDPE in %	Wood in %	CaCO3	MAPE
HDPEr 30W70	30	70	-	-
HDPEr30W59CC7	30	59	7	4
HDPEr40W60	40	60	-	-
HDPEr40W49CC7	40	49	7	4
HDPEr50W50	50	50	-	-
HDPEr50W39CC7	50	39	7	4
HDPEr60W40	60	40	-	-
HDPEr60W29CC7	60	29	7	4
HDPEr70W30	70	30	-	-
HDPEr70W19CC7	70	19	7	4

That W, HDPEr and CC codes were used to refer to wood flour, recycled high-density polyethylene and calcium carbonate $CaCO_3$, respectively

Dimensional stability tests

According to ASTM D570-98 (ASTM 2002b), a water absorption investigation on several wood–plastic panels (WPC) was carried out. The specimens were submerged in water for 2 and 24 h at a temperature of 23 ± 1 °C, and measurements and weight were taken 20 min after they were taken out of the water.

The mass loss of a sample between its initial state and its state after being dried in an oven at 105 °C for 24 h was weighed to determine the moisture content. The relationship between the mass loss and moisture is as follows:

$$H\% = \frac{M_h - M_0}{M_0} \times 100 \quad (1)$$

with M_h: The mass of the specimen in the wet state; M_0: The mass of the specimen in the anhydrous state.

The density of the composite cannot be constant for a given moisture content; rather, it varies with humidity; as a result, it is represented for a certain moisture level H%. The following relation was used to calculate the density of the composite in the anhydrous state:

$$D_0 = \frac{M_0}{V_0} \quad (2)$$

with M_0: The mass of the specimen in the anhydrous state; V_0: The volume of the specimen in the anhydrous state.

The relative rise in the sample's size (length) in all three dimensions (radial (R), tangential (T) and longitudinal (L)) is known as linear swelling. The following relationship has been employed to quantify the increase in wood moisture

$$G_l\% = \frac{L_s^i - L_0^i}{L_0^i} \times 100 \quad (3)$$

Table 2 Absorption of water and swelling of the thickness of wood–plastic composites

Samples	Density kg/m^3	Moisture absorption (%)				Thickness swelling (%)			E-type
		2 h	E-type	24 h	E-type	2 h	E-type	24 h	
HDPEr30W70	1053	2.91	0.0713	5.21	0.1123	1.53	0.0545	2.91	0.0812
HDPEr30W59CC7	1078	1.46	0.0712	2.72	0.1097	0.77	0.088	1.47	0.0811
HDPEr40W60	1021	2.25	0.0707	4.12	0.0707	1.23	0.0875	2.33	0.0806
HDPEr40W49CC7	1043	1.13	0.0687	2.05	0.0687	0.51	0.0855	1.17	0.0786
HDPEr50W50	998	1.83	0.0686	3.91	0.0686	0.82	0.0854	1.94	0.0785
HDPEr50W39CC7	1012	0.92	0.0656	1.98	0.0656	0.42	0.0824	0.98	0.0755
HDPEr60W40	980	0.96	0.0672	2.20	0.0672	0.57	0.084	1.62	0.0771
HDPEr60W29CC7	997	0.49	0.0624	1.15	0.0624	0.27	0.0792	0.82	0.0723
HDPEr70W30	962	0.42	0.0619	0.97	0.0619	0.29	0.0787	0.44	0.0718
HDPEr70W19CC7	983	0.23	0.0609	0.51	0.0609	0.15	0.0777	0.22	0.0708

*E-type is to indicate that all the components are unidirectional and CC stands for $CaCO_3$

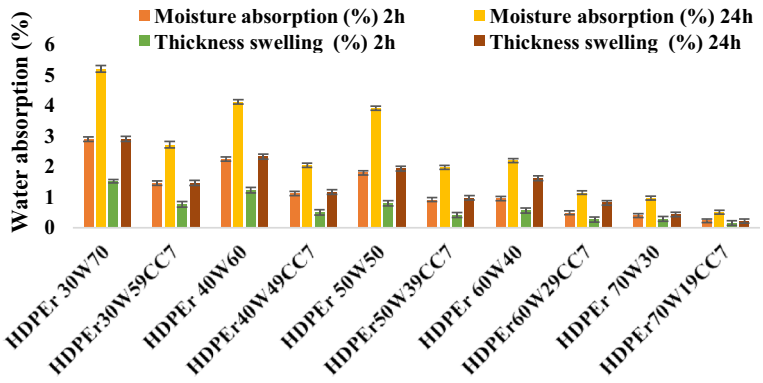

Fig. 1 Water absorption and swelling in thicknesses for 2 h and 24 h for the different composite formulations

Table 3 Mechanical properties of the different formulations of WPC composites

Samples	Tensiles trength(MPa)	E-type	Tensile modul(GPa)	E-type	Flexural strength(MPa)	E-type	Flexural modul(GPa)	E-type
HDPEr30W70	07.75	0.598	1.078	0.034	17.31	0.623	2.462	0.057
HDPEr30W59CC7	13.54	0.564	1.321	0.032	28.69	0.587	2.794	0.054
HDPEr40W60	10.53	0.591	1.057	0.028	19.99	0.51	2.364	0.051
HDPEr40W49CC7	16.75	0.524	1.219	0.025	31.22	0.451	2.743	0.048
HDPEr50W50	13.57	0.493	1.041	0.022	23.32	0.427	2.218	0.046
HDPEr50W39CC7	19.01	0.455	1.131	0.018	33.46	0.364	2.711	0.043
HDPEr60W40	15.42	0.363	1.033	0.016	25.69	0.343	2.141	0.042
HDPEr60W29CC7	20.23	0.345	1.101	0.013	34.89	0.301	2.647	0.037
HDPEr70W30	18.42	0.302	1.025	0.011	28.99	0.256	2.052	0.035
HDPEr70W19CC7	24.10	0.254	1.087	0.008	37.41	0.232	2.571	0.031

with *L*: Dimension (length); *i*: *R*, *T* or *L*; *s*: Saturated state; 0: Anhydrous state at 105 °C.

Tensile and flexural tests

Using a universal testing machine (Instron, model 8112), mechanical properties of WPCs were tested under flexural and tensile conditions in accordance with ASTM D790 and D638, respectively. For the tensile and flexural tests, the

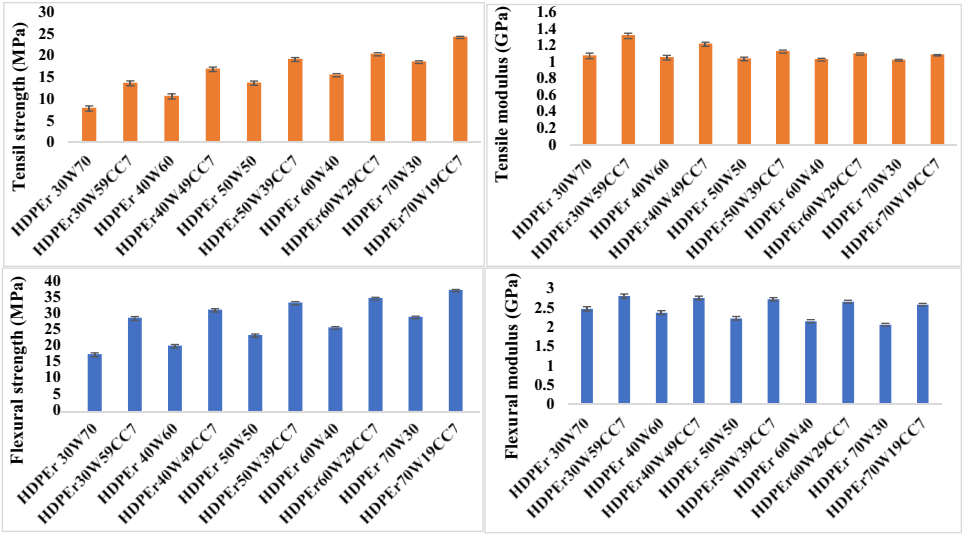

Fig. 2 Mechanical properties of the different formulations of WPC composites

specimens were evaluated at room temperature at crosshead speeds of 5 mm/min according to ASTM standards. The mechanical test was performed according to ASTM D1037 standards on WPC panels with dimensions 250 × 80 × 10 mm^3complied. All of the test results that were published were the averages of five different specimens.

X-ray diffraction

Samples from the different WPC composites were analyzed by X-ray diffraction (Semen's D500) with Cu Kα radiation (l = 1.24056 Å). To identify the crystalline phases, the used a scanning range is of 10–55 with a pitch of 0.04 recorded every 5 s.

Surface analysis by water contact angle measurements

The contact angle was directly measured by scanning the 30 s droplet profile using the high-resolution position Camera CCD 'CAM-200 from KSV-Finland', the profile of liquid droplets located on the composites surface with a 3.2 version screen reporter software from Iconic Inc., New York, NY, USA. Then, the angle was calculated from the dimensions of the droplet imager, using digital image analysis software developed and distributed free of charge by STEM Education Institute, University of Massachusetts Amherst, USA), and the following relationship:

$$\theta = 2.\mathrm{Arctg}\left(\frac{2h}{d}\right) \quad (4)$$

where h and d Stand for the droplet's height and length, respectively.

SEM analysis

The scanning electron microscope is equipped with a secondary electron detector, a backscattered electron detector and requires a secondary vacuum in the observation chamber (10–6 mbar). SEM was performed on 30 × 4 × 3 mm^3 samples to visualize the wood/plastic interface and to draw conclusions about the homogeneity of the obtained composite panels. Samples were analyzed at 100× magnification.

Results and discussion

Moisture absorption and thickness swelling

The results of the composite density, moisture absorption and swelling of the different WPC composites as well as the control samples are summarized in Table 2.

It is concluded from the results that the density of the composites increases due to the increase in wood content in the matrix, and composites containing calcium carbonate have a higher density than the control samples. The addition of 4% by weight of MAPE also improves the interfacial compatibility between the polymer matrix and wood powder (Arman et al. 2021). It is also note that the water absorption increases with the increase in the wood content in the composite, the behavior is almost the same for the tests of immersion in water for durations of 2 h and 24 h. The use of the $CaCO_3$ and the MAPP reduces the absorption by almost 7%. Indeed, higher plastic composites have fewer water absorption sites, resulting in lower water absorption. The swelling (TS) of WPC composites follows a similar pattern of water absorption. The TS values for 2 h

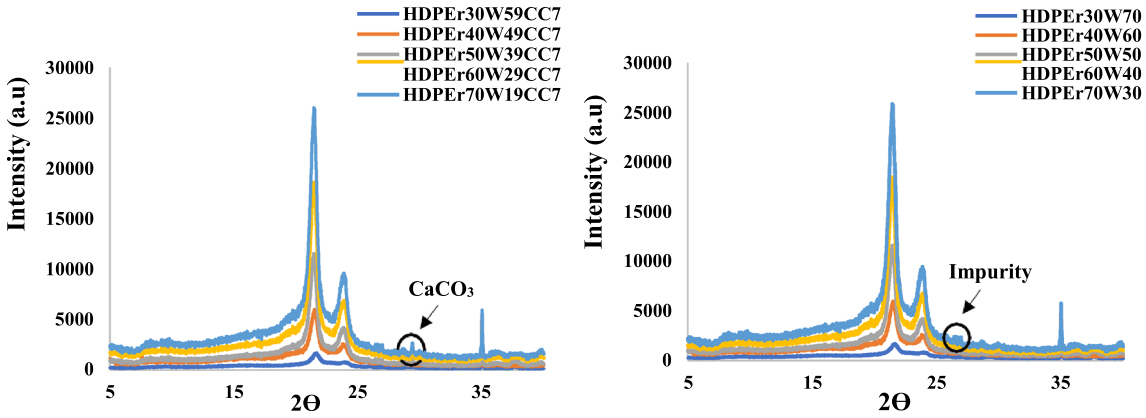

Fig. 3 XRD patterns of different WPC composite formulations with or without the addition of CaCO3

Table 4 Experimental and theoretical measurement of contact angles of WPCr composites (Lazrak et al. 2019)

CSamples	θ (Measured)	θ = Arctg ((2 h/d))	
HDPEr70B30	67.63	h = 24	68.12
		d = 71	
HDPEr70W19CC7	69.96	h = 25	71.07
		d = 70	
HDPEr60W40	64.11	h = 23	65.14
		d = 72	
HDPEr60W29CC7	66.89	h = 24	68.12
		d = 71	
HDPEr50W50	53.76	h = 20	56.78
		d = 74	
HDPEr50W39CC7	55.85	h = 20	56.78
		d = 74	
HDPEr40W60	49.02	h = 18	51.28
		d = 75	
HDPEr40W49CC7	52.22	h = 19	53.13
		d = 76	
HDPEr30W70	33.97	h = 15	34.37
		d = 97	
HDPEr30W59CC7	35.02	h = 15	36.86
		d = 90	

Underline values indicate the experimental and theoretical measurement of contact angles of WPCr composites

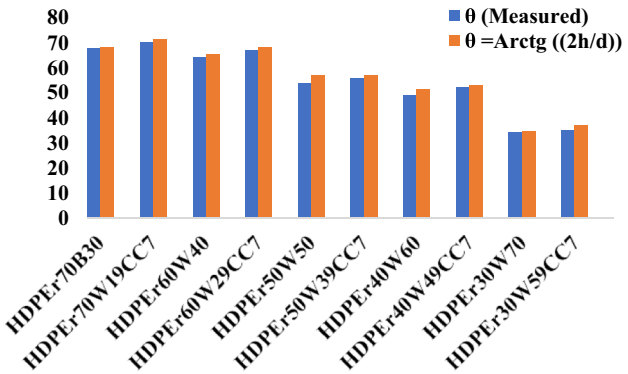

Fig. 4 Measured and calculated contact angle of different WPC composites

immersion in water vary from 0.15 to 1.53%, and these values are increased after 24 h immersion, varying from 0.22 to 2.91% (Fig. 1).

Tensile and flexural of composites WPC

The tensile and flexural strength module results for the different formulations of the WPC composites as well as the control samples are summarized in Table 3.

It is well observed from Fig. 2 that tensile strength is improved with the decrease in wood powder content in the polymer matrix, and with the addition of 7% by weight of $CaCO_3$ and 4% by weight of MAPE. This improvement is likely attributed to improved polymer wood interactions with the addition of the coupling agent and the $CaCO_3$ loading (Srivabut et al. 2021; Wang 2021). The highest tensile strength value was recorded for the HDPEr70W19CC7 sample with a value of 24.1 MPa. The control samples recorded lower values for the same percentage of recycled HDPE. The lowest tensile strength value was recorded for the control sample HDPEr 30W70 with a value of 7.75 MPa. In contrast to tensile strength, the tensile module increases with the addition of higher wood powder content in the polymer matrix. According to Fig. 2, the highest value of the traction modulus was recorded for the HDPEr30W59CC7 sample with a value of 1.321 GPa, the addition of 7% in load weight and 4% in weight of MAPE to contribute to the improvement of the traction modulus (Srivabut et al. 2022), It is more probably that 4% MAPE has filled the voids between the grainis of the composite and this is clearly shown by the enhancement of the density which gives us an idea about how

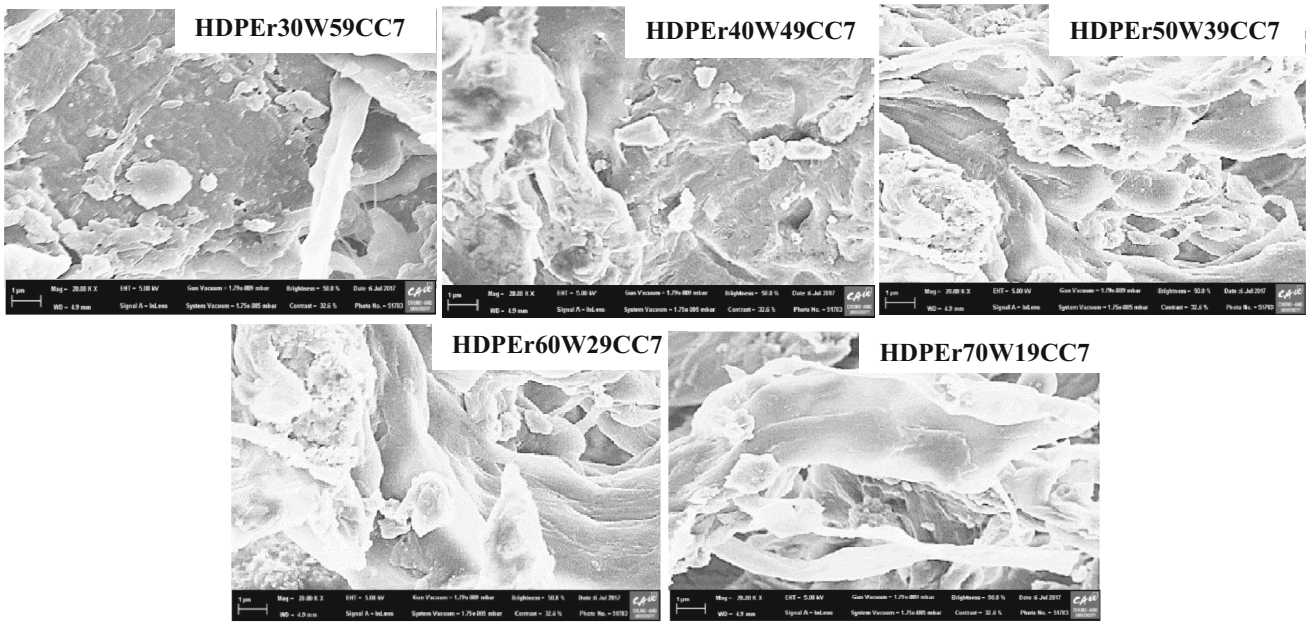

Fig. 5 Interfacial micrographs of the five fabricated specimens

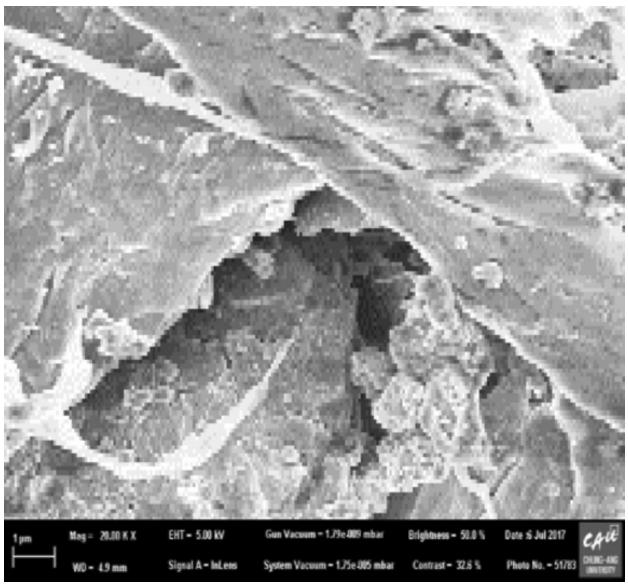

Fig. 6 Fracture surface micrograph of (HDPEr50W50)

reduced the porosity rate would become. The control samples recorded a module inferior to the WPC composites for the same polymer percentage. The lowest value was recorded for control sample 1.025 GPa.

Furthermore, it is noticed from Fig. 2 that flexural strength follows the same trend as the tensile strength. In fact, flexural strength increases with the decrease in the wood content in the polymer matrix. Maximum values were recorded for samples containing 7% by weight of load and 4% by weight of MAPE (Ali et al. 2020). The highest value was recorded for the HDPEr70W19CC7 sample with a value of 37.41 MPa. The control samples recorded minimum values. The lowest value was recorded for the HDPEr30W70 control sample with a value of 17.31 MPa. It is also note that the flexural module increases with the increase in wood content in WPC composites. The highest values are recorded for samples proceeding 7% by weight of $CaCO_3$. The highest value was recorded for HDPEr30W59CC7 samples with a value of 2.794 GPa and a minimum value for the HDPEr70W30 control sample with a value of 2.052 GPa. This trend follows perfectly the literature (Techawinyutham et al. 2021).

X-ray diffractometry (XRD) analysis

According to Fig. 3, the XRD patterns of all WPC are similar for the same sample compositions, but peak intensity depends on the formulation of the WPC. The maximum 2Θ reflection values correspond to the crystallographic planes of cellulose, recycled polymer and $CaCO_3$ (Echeverria et al. 2020; Assaedi 2021). For WPC composites containing $CaCO_3$, the characteristic crystal band of $CaCO_3$ was observed at reflection $2\theta = 29.40°$ with a low intensity that reflects the low percentage of $CaCO_3$ in WPC (Xian et al. 2015). In addition, the crystalline bands characteristic of HDPEr were observed at several reflections, three bands of high intensities $2\theta = 21.4°$; $2\theta = 24.0°$; $2\theta = 35.0°$; and a single band of low intensities $2\theta = 20.0°$ (Lazrak et al. 2019).

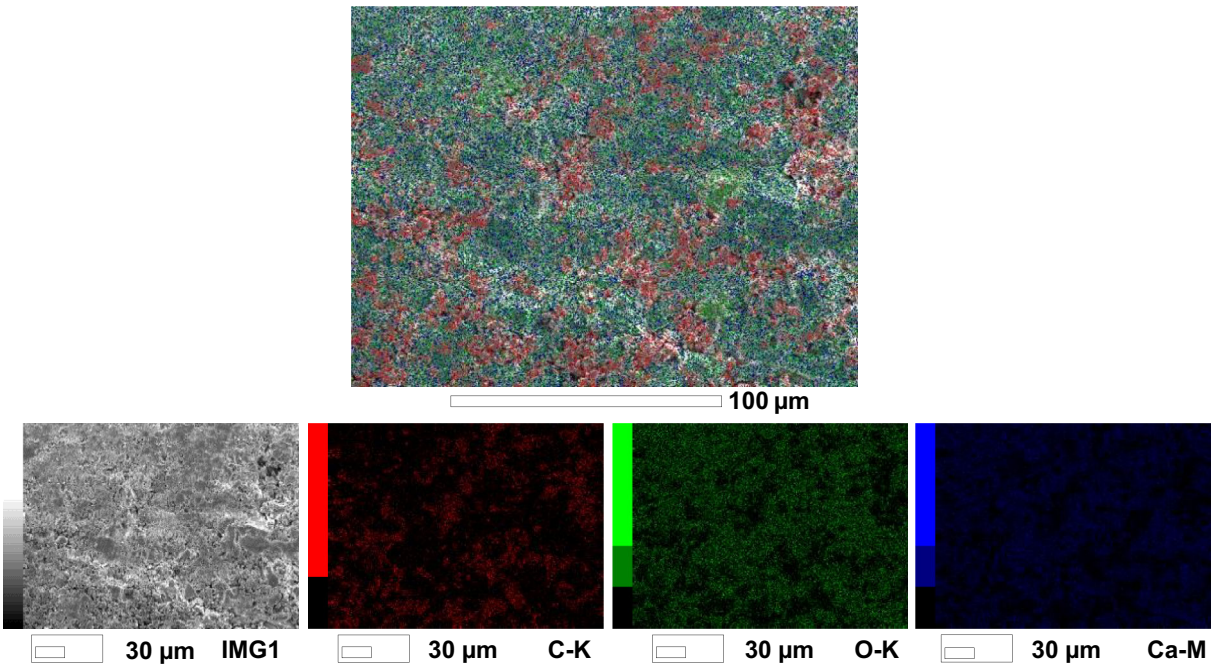

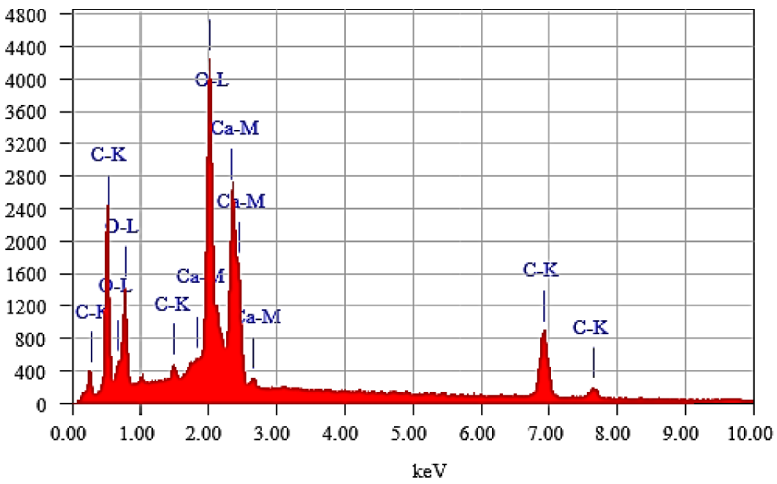

ZAF Method Standard less Quantitative Analysis
Fitting Coefficient: 0.2003

Element	(keV)	mass%	Error%	At%	Compound	mass% Cation	K
C K	3.776	21.04	0.06	25.56			1.1148
O L	11.525	43.17	0.06	66.75			17.7974
Al K	1.486	0.61	0.07	0.90			0.4871
Ca M	2.342	35.18	0.30	6.79			30.9943
Total		100.00		100.00			

Fig. 7 SEM micrograph along with EDX elemental maps

Surface analysis by water contact angle measurements

To determine the hydrophobic characteristics of the WPC surfaces, the contact angle measurements were carried out. For this, the technique used is the sessile drop (Xian et al. 2022). The results of the surface condition and hydrophobicity study of WPC composites with different formulations with or without $CaCO_3$ are summarized in Table 4. The contact angle was calculated in two ways: the experimental method of measuring the contact angle from the sessile drop at room temperature and the theoretical method. It was noticed that the surface of the composite containing a high polyethylene content and with the addition of 7% by weight of $CaCO_3$ indicates a hydrophobic

behavior at an angle of 69.96. This contact angle is attributed to the presence of polyethylene and $CaCO_3$ on the surface of the WPC composite (Cao et al. 2016). Composites that do not contain a percentage of charge have a lower angle of contact per intake to those that contain 7% by weight of $CaCO_3$ are those for the same formulations. The lowest contact angle value was recorded for the HDPEr30W70 with a value of 33.97°. This also means that the increase in wood content increases the hygrophyly on the surface of the WPC. Indeed, the decrease in the contact angle is due to the increase in the roughness of the surface, which results from the increase in the wood content in the polymer matrix, therefore the drop of water expands immediately, and this is in good agreement with the morphological studies (Nukala et al. 2022).

The comparative study of the measured and calculated contact angle (Figs. 4) shows a good agreement, which means that our developed method is valid.

SEM analysis

The microstructure of the WPC composite in its initial state (after incorporation) is observed using a scanning electron microscope shown in Fig. 5, the HDPEr matrix is recognized (dark), and wood particles (light gray) as well as the pores produced during the manufacturing process. SEM micrographs have different microstructures of different WPC composite formulations ranging from 30% by weight to 70% by weight of wood. HDPEr-wood flour composites with a load of 30 wt% are shown in Fig. 5 where many cavities are observed. The presence of these cavities confirms that the interfacial bond between the mouth-pores and the polymer matrix is weak. In addition, localized piles of wood and HDPEr matrix plates are observed, indicating poor dispersion of loads in the HDPEr bed. When the wood content is increased, the polymer matrix is no longer continuously distributed and many wood fibers are in direct contact with each other, resulting in poor bonding of the adhesion to the interface.

It should be noted that the pores are gradually decreased by increasing the wood content in the plastic matrix, which explains the reduced density of WPC containing less amount of HDPEr, this behavior is in great agreement with the density results. Figure 6 shows the micrograph of the composite fracture surface filled with 50 wt% of wood floor. The SEM image shows that there is no clear space between the wood floors and the HDPEr matrix, indicating the good interface connection.

In order to learn more about the topography of the composites, the element mapping image was performed. After sputtering the sample with Au/Pd alloy, the studied sample was examined at a higher magnification (× 2000) using a scanning electron microscope of the JEOL JED 2300 type outfitted with a 6380 LA EDX analyzer with the sample set up at 512 × 384 points and individual spectra recorded for as long as 0.1 ms per point, digital X-ray maps were created.

Figure 7 displays the EDX elemental maps and SEM micrograph of HDPEr50W39CC7. According to SEM maps, the examined composition is made entirely of the components C, Ca and O. This result offers convincing proof that the WPC composites were effectively created with a consistent distribution of $CaCO_3$ throughout the matrix. The elemental map of the sample shows the presence of $CaCO_3$ (blue dots) within the matrix. Indeed, elemental mapping by scanning electron microscopy and its corresponding EDX spectroscopy confirmed that the $CaCO_3$ fillers were embedded in the matrix by partially occupying the existing cavities and that their distribution was almost uniform. Also, as shown, the EDS spectrum shows traces of isolated Al and C. They represent impurities. Finally, the investigation of the surface by SEM mapping has clearly indicated the filler/matrix interface. The latter may lead to some filler-matrix interactions; as shown above, $CaCO_3$ filler plays a reinforcing role.

Conclusions

The present work has led to the following conclusions:

The hot-press composites have very low water absorption and thickness swelling, making the products stable in humid environments. Water absorption and thickness swelling, on the other hand, increase with wood content.

Because of increased interfacial bonding, composites containing 50% recycled plastic have high stability qualities.

Tensile and flexural tests were used to determine the mechanical characteristics of the composites. The composites with lesser wood content have lower rigidity, and the composite with 50% reused plastic has moderated tensile and flexural strength. As a result of its superior stability and mechanical qualities, this composite is anticipated to be the most useful material.

Funding AcknowledgmentsThis research received no external funding

Declarations

Conflict of interest The authors declare no conflict of interest.

References

Aina KS, Oladimeji AO, Agboola FZ, Oguntayo DO (2022) Dimensional stability and mechanical properties of extruded-compression biopolymer composites made from selected Nigerian grown wood species at varying proportions. Sci Rep 12(1):1–11. https://doi.org/10.1038/s41598-022-14691-z

Ali SFA, El Batouti M, Abdelhamed M, El-Rafey E (2020) Formulation and characterization of new ternary stable composites: polyvinyl chloride-wood flour-calcium carbonate of promising physicochemical properties. J Mater Res Technol 9(6):12840–12854. https://doi.org/10.1016/j.jmrt.2020.08.113

American Society for Testing and Materials (ASTM). ASTM D618-99: In: 2002 Annual book of ASTM Standards. ASTM, West Conshohocken

American Society for Testing and Materials (ASTM). ASTM D570-98: In: 2002 Annual book of ASTM Standards. ASTM, West Conshohocken

Amiandamhen SO, Meincken M, Tyhoda L (2020) Natural fibre modification and its influence on fibre-matrix interfacial properties in biocomposite materials. Fibers Polym 21(4):677–689. https://doi.org/10.1007/s12221-020-9362-5

Antônio dos Santos Filho E, Bruno Barreto Luna C, Diniz Siqueira D, Andrade dos Santos Nogueira J, Maria Araújo E (2021) Reuse of carbon fiber waste to produce composites with polypropylene. The effect of styrene-(ethylene-butylene)-styrene grafted with maleic anhydride and ethylene-propylene-diene grafted with maleic anhydride copolymers. Polym Compos 42(11):6182–6195. https://doi.org/10.1002/pc.26295

Arman NSN, Chen RS, Ahmad S (2021) Review of state-of-the-art studies on the water absorption capacity of agricultural fiber-reinforced polymer composites for sustainable construction. Constr Build Mater 302:124174. https://doi.org/10.1016/j.conbuildmat.2021.124174

Assaedi H (2021) The role of nano-$CaCO_3$ in the mechanical performance of polyvinyl alcohol fibre-reinforced geopolymer composites. CompositeInterfaces 28(5):527–542. https://doi.org/10.1080/09276440.2020.1793096

Borysiuk P, Wilkowski J, Krajewski K, Auriga R, Skomorucha A, Auriga A (2020) Selected properties of flat- pressed wood-polymer composites for high humidity conditions. BioResources 15(3):5141–5155

Cao Z, Daly M, Clémence L, Geever LM, Major I, Higginbotham CL, Devine DM (2016) Chemical surface modification of calcium carbonate particles with stearic acid using different treating methods. Appl Surf Sci 378:320–329. https://doi.org/10.1016/j.apsusc.2016.03.205

Echeverria CA, Pahlevani F, Sahajwalla V (2020) Valorisation of discarded nonwoven polypropylene as potential matrix-phase for thermoplastic-lignocellulose hybrid material engineered for building applications. J Clean Prod 258:120730. https://doi.org/10.1016/j.jclepro.2020.120730

Elamin MAM, Osman ZA, Otitoju TA (2020) Preparation and characterization of wood-plastic composite by utilizing a hybrid compatibilizer system. Ind Crops Prod 154:112659. https://doi.org/10.1016/j.indcrop.2020.112659

Friedrich D (2021) Thermoplastic moulding of wood-polymer composites (WPC): a review on physical and mechanical behaviour under hot-pressing technique. Compos Struct 262:113649. https://doi.org/10.1016/j.compstruct.2021.113649

Homkhiew C, Rawangwong S, Boonchouytan W, Suchaiya V (2022) Morphological, mechanical, and physical properties of ground rubber tire thermoplastic elastomer/rubberwood sawdust composites: effects of composition contents and rubber types. J Thermoplastic Compos Mater. https://doi.org/10.1177/08927057221086834

Kamarudin SH, Mohd Basri MS, Rayung M, Abu F, Ahmad SB, Norizan MN, Osman S, Sarifuddin N, Desa MS, Abdullah UH, Mohamed Amin Tawakkal IS (2022) A review on natural fiber reinforced polymer composites (NFRPC) for sustainable industrial applications. Polymers 14(17):3698. https://doi.org/10.3390/polym14173698

Kuo PY, Wang SY, Chen JH, Hsueh HC, Tsai MJ (2009) Effects of material compositions on the mechanical properties of wood–plastic composites manufactured by injection molding. Mater Des 30(9):3489–3496. https://doi.org/10.1016/j.matdes.2009.03.012

Lazrak C, Kabouchi B, Hammi M, Famiri A, Ziani M (2019) Structural study of maritime pine wood and recycled high-density polyethylene (HDPEr) plastic composite using Infrared-ATR spectroscopy, X-ray diffraction, SEM and contact angle measurements. Case Stud Constr Mater 10:e00227. https://doi.org/10.1016/j.cscm2019.e00227

Mandal M, Gogoi G, Dutta N, Maji TK (2021) Development of biobased wood polymer nanocomposites: industrial applications, market, and future trends. In: Hussain CM (ed) Handbook of polymer nanocomposites for industrial applications. Elsevier, Amsterdam, pp 587–615. https://doi.org/10.1016/B978-0-12-821497-8.00022-8

Maraveas C (2020) Production of sustainable and biodegradable polymers from agricultural waste. Polymers 12(5):1127. https://doi.org/10.3390/polym12051127

Nukala SG, Kong I, Kakarla AB, Tshai KY, Kong W (2022) Preparation and characterisation of wood polymer composites using sustainable raw materials. Polymers 14(15):3183. https://doi.org/10.3390/polym14153183

Nur-A-Tomal MS, Pahlevani F, Sahajwalla V (2022) Study on the direct transformation of milk bottle and wood into wood–plastic composite through injection molding. J Compos Sci 6(8):230. https://doi.org/10.3390/jcs6080230

Ratanawilai T, Srivabut C (2022) Physico-mechanical properties and long-term creep behavior of wood–plastic composites for construction materials: effect of water immersion times. Case Stud Constr Mater 16:e00791. https://doi.org/10.1016/j.cscm.2021.e00791

Roig I (2018) Biocomposites for interior facades and partitions to improve air quality in new buildings and restorations. Reinf Plast 62(5):270–274. https://doi.org/10.1016/j.repl.2017.07.003

Srivabut C, Ratanawilai T, Hiziroglu S (2018) Effect of nanoclay, talcum, and calcium carbonate as filler on properties of composites manufactured from recycled polypropylene and rubberwood fiber. Constr Build Mater 162:450–458. https://doi.org/10.1016/j.conbuildmat.2017.12.048

Srivabut C, Ratanawilai T, Hiziroglu S (2021) Statistical modeling and response surface optimization on natural weathering of wood–plastic composites with calcium carbonate filler. J Mater Cycles Waste Manage 23(4):1503–1517. https://doi.org/10.1007/s10163-021-01230-7

Srivabut C, Ratanawilai T, Hiziroglu S (2022) Response surface optimization and statistical analysis of composites made from calcium carbonate filler-added recycled polypropylene and rubberwood fiber. J Thermoplast Compos Mater 35(3):391–415. https://doi.org/10.1177/0892705719889988

Techawinyutham L, Sumrith N, Srisuk R, Techawinyutham W, Siengchin S, MavinkereRangappa S (2021) Thermo-mechanical, rheological and morphology properties of polypropylene composites: residual $CaCO_3$ as a sustainable by-product. Polym Compos 42(9):4643–4659. https://doi.org/10.1002/pc.26175

Wang Y (2021) Mechanical properties effect of wood-plastic composite by basalt fiber and MAPE. In: IOP Conference series:

earth and environmental science, 726(1):012005. https://doi.org/10.1088/1755-1315/726/1/012005.

Xian Y, Li H, Wang C, Wang G, Ren W, Cheng H (2015) Effect of white mud as a second filler on the mechanical and thermal properties of bamboo residue fiber/polyethylene composites. BioResources 10(3):4263–4276

Xian Y, Wang C, Wang G, Smith L, Cheng H (2022) The influence of white mud on the water absorption, surface wettability, mechanical, and dynamic thermomechanical properties of core–shell structured wood-plastic composites. Eur J Wood Wood Prod 80(2):355–365. https://doi.org/10.1007/s00107-021-01772-5

Xu B, Wei MY, Wu XY, Fu LY, Luo F, Lei JG (2021) fabrication of micro-groove on the surface of CFRP to enhance the connection strength of composite part. Polymers 13(22):4039. https://doi.org/10.3390/polym13224039